JOURNAL OF MATERIALS SCIENCE **37** (2002) 3035–3043

Study on the formation and growth of potassium titanate whiskers

NINGZHONG BAO, XIN FENG, XIAOHUA LU*, ZHUHONG YANG
Department of Chemical Engineering, Nanjing University of Chemical Technology, Nanjing, Jiangsu, 210009, People's Republic of China
E-mail: xhlu@njuct.edu.cn

In this paper, $K_2Ti_2O_5$ single crystals, $K_2Ti_4O_9$ whiskers and $K_2Ti_6O_{13}$ whiskers are synthesized form the anatase-K_2CO_3 starting materials by the heating calcination and the corresponding morphologic and structural evolution of products are observed. After dissolving non-crystalline hydrosoluble products contained in sinters, the morphologic difference between the original sinter and the whiskers in it shows the sinter microstructure. The further analysis to crystal components in sinters and to the phase diagram proves that $K_2Ti_4O_9$ whiskers are firstly formed in $K_2Ti_2O_5$ crystals and there only exists the phase transformation from $K_2Ti_4O_9$ whiskers with layered crystal structure to $K_2Ti_6O_{13}$ whiskers with tunnel crystal structure. The K_2O-rich liquid melt generated from $K_2Ti_2O_5$ crystals (/and $K_2Ti_4O_9$ whiskers) coats on the surface of $K_2Ti_4O_9$ whiskers (/and $K_2Ti_6O_{13}$ whiskers), which makes the sinters taking on the layer-by-layer structure (/and the bunch structure). The formation and growth of whiskers is dictated by the K_2O-rich non-crystalline hydrosoluble melt generated in phase transformations from solid to liquid-solid and its split effect induced by the orientation melting. A generalized "liquid melt inducing" mechanistic model explaining the formation and growth of potassium titanate whiskers was proposed.

1. Introduction

Potassium titanate whiskers expressed by $K_2O \cdot nTiO_2$ (wherein $n = 2$, 4 or 6) or expressed by $K_2Ti_2O_5$, $K_2Ti_4O_9$ and $K_2Ti_6O_{13}$ [1, 2] are usually prepared by the calcination method and mainly used as a reinforcing agent to prepare high-performance plastics [3, 4], ceramics [5–7] and so on. Furthermore, the strong ion-exchange properties for potassium titanate whiskers provide an excellent method to prepare the fibrous titanium dioxide or mixed metal titania fibers [2, 8–12] that are difficult to be directly synthesized by the traditional chemical synthesis and can be valuable as supporters [13], sensors [14, 15], ionic conductors [16] and photocatalysts [17–19]. The fibrous or whisker's morphology plays the key role in the wide applications of potassium titanate whiskers.

The morphologic control is a difficult and challenging topic in the material synthesis and products with different morphologies, such as grain and whisker may be prepared under different synthesis conditions [20–22]. Some research works have been done on the formation and growth of potassium titanate whiskers. Lee *et al*. [23] and Fujiki *et al*. [24] studied the growth of potassium titanate whiskers and corresponding reactions taken place in the slow-cooling calcination process. Lee *et al*. [23] further observed the morphologic evolution from the rod-like $K_2Ti_6O_{13}$ to the $K_2Ti_4O_9$ whisker at the calcination temperature above 950°C. However, reactions and the microstructural evolution from the starting materials of the powder mixture of anatase and K_2CO_3 to $K_2Ti_6O_{13}$ whiskers in heating calcination were not studied. Fujiki *et al*. [24] only reported the chemical component change and did not study the morphologic evolution of products. Shimizu [25] found that the morphologies and components of products are determined by the calcination temperature and the TiO_2/K_2CO_3 molar ratio of staring materials. However, no detailed and full research was done to discover the relation between the morphology and the chemical components of products so that the formation and growth of potassium titanate whiskers is still not clear. The existing mechanisms of the formation and growth of whiskers, such as VL [26] and VLS [27], do not agree with the experimental phenomena appearing in the heating-calcination synthesis of potassium titanate whiskers. Based on the experimental evidence obtained with various methods such as X-ray diffraction and scanning electron microscopy, previous studies [23–25] only reported the information about the final crystal products and relatively optimum synthesis conditions of the whiskers.

In order to control the product morphologies the formation and growth of potassium titanate whiskers should be deeply understood. Phase diagram [1, 28]

*Author to whom all correspondence should be addressed.

shows that there exist different phase equilibriums and transformations among different types of potassium titanates at corresponding reaction temperatures in heating calcination. Here we report a direct, micrograph evidence and method of microstructure and morphology to fully understand the formation and growth of potassium titanate whiskers in heating calcination.

2. Experimental section

2.1. Sampling and sintering process

Starting materials, K_2CO_3 and nano TiO_2 (anatase) powders (All reagent grade, Shanghai Chemical Agent Plant, P. R. China), were well mixed by adding a certain water and surfactants. Powder mixtures were then pressed into 20 mm × 20 mm × 10 mm disks and dried in an oven at 100°C for 10 h. The disks were sintered at corresponding calcination temperatures for 10 h, and taken out at the end of calcinations immediately and then cooled in air. Detailed experimental conditions for all samples of A1–F1 and A2–F2 appearing in the following text are shown in Table I.

Temperature control for a muffle furnace (Model SX2-2.5-12, Nanjing High-temperature Service Plant, P. R. China) with a 20 cm × 12 cm × 8 cm (length × width × height) heating chamber was done by the instrument (Model AI-708, Xiameng Yuguang Electronic Technology Institute, P. R. China) at the temperature fluctuation range of ±2°C and at the heating rate of 10°C/minute.

2.2. Identification of crystalline phase

Crystalline phases were subject to powder X-ray diffraction obtained on a DMAX-B (Rigaku Denki Corp., Tokyo, Japan) using Ni-filtered Cu K_α ($\lambda =$ 1.54178 Å) radiation, operating at 40 kV and 100 mA, respectively. Powder samples (40–80 mg) were measured in continuous scanning mode from 5°–80° (2θ) at the scanning rate of 0.02° (2θ)/second. Peak positions and relative intensities were characterized by the comparison to standard Joint Committee on Powder Diffraction and Standards (JCPDS) files.

TABLE I Synthesis conditions and crystal components in products

Sample[a]		TiO_2/K_2O molar ratio	React. temp. (°C)	Crystal component[b]
A	A1	3.0	710	TiO_2
	A2			TiO_2
B	B1	3.0	830	$K_2Ti_2O_5$
	B2			$K_2Ti_2O_5$
C	C1	3.0	960	$K_2Ti_4O_9$
	C2			$K_2Ti_4O_9$
D	D1	3.0	1130	$K_2Ti_6O_{13}$
	D2			$K_2Ti_6O_{13}$
E	E1	3.9	960	$K_2Ti_4O_9$
	E2			$K_2Ti_4O_9$
F	F1	5.9	1130	$K_2Ti_6O_{13}$
	F2			$K_2Ti_6O_{13}$

[a]Sinter products for A, B, C, D, E and F were divided into two parts. A1, B1, C1, D1, E1 and F1 were immersed and dispersed in the ethanol for keeping the original morphology and the surface condition of sinters. A2, B2, C2, D2, E2 and F2 were leached and disassembled in boiling water to dissolve the non-crystalline hydrosoluble products for observing the morphologies of the crystal products and the sinter structure.
[b]Decided by XRD test.

2.3. Morphologic and microstructural evolution studies of products

For the same sample listed in Table I as well as A–F was divided into two parts. One part as well as A1–F1 was immersed and dispersed in the ethanol to prevent the hydrosoluble products form dissolving and thus to keep the original morphology and the surface condition of sinters; another part as well as A2–F2 was leached and disassembled in boiling water for two hours to dissolve the non-crystalline hydrosoluble products and thus to expose the sinter structure and the morphologies of the crystal products. Their Morphologies and microstructures were then observed by the optical microscope (Model Galen III, Jiangnan Optical Instrument Co., Ltd., P. R. China). The surface morphology was examined by scanning electron microscope (SEM) (JSM-6300, JEOL, Japan)

3. Results

3.1. Results of XRD test

Table I lists the synthesis conditions and the corresponding crystal phase components determined by XRD test. It can be found that $K_2Ti_2O_5$, $K_2Ti_4O_9$ and $K_2Ti_6O_{13}$ are synthesized from starting materials of TiO_2 and K_2CO_3 with different TiO_2/K_2O molar ratio at 830°C, 960°C and 1130°C, respectively. Their characteristic peaks and the relative intensities were characterized by comparing to JCPDS files and also show good agreement with the data reported [29–31].

3.2. Morphologies of sinters and corresponding crystal products

Fig. 1 shows the morphologies and microstructures of sinters and corresponding dispersed crystal products generated at heating calcination.

From Fig. 1 it is find that sinter products generated at different reaction stages have their special morphologies. A1 and A2 are gain agglomerations and dispersed gains, respectively. Also, crystal products in both A1 and A2 are crystal TiO_2 knowing from Table I, indicating that K_2CO_3 was decomposed into hydrosoluble non-crystal K_2O at 710°C and no reaction is taken place with sphere-like TiO_2 particles that can be easily dispersed in boiling water. Knowing from Table I and Fig. 1 crystal products in both B1 and B2 are $K_2Ti_2O_5$ single crystals with the same size, morphology and clean surface, indicating that at 830°C the crystal products are thick $K_2Ti_2O_5$ single crystals and no hydrosoluble product is generated. Crystal products in both C1 and C2 are $K_2Ti_4O_9$ whiskers. Sinters of C1 have the unclean surface and are easily broken into whiskers with smooth surface as shown in C2 in boiling water, indicating that at 960°C sinters of C1 is composed of the $K_2Ti_4O_9$ whisker sheaves and the non-crystalline hydrosoluble products covering on the whisker surface. Furthermore, whisker sheaves of C1 share the close size with that of the single crystals of B1. At 1130°C both D1

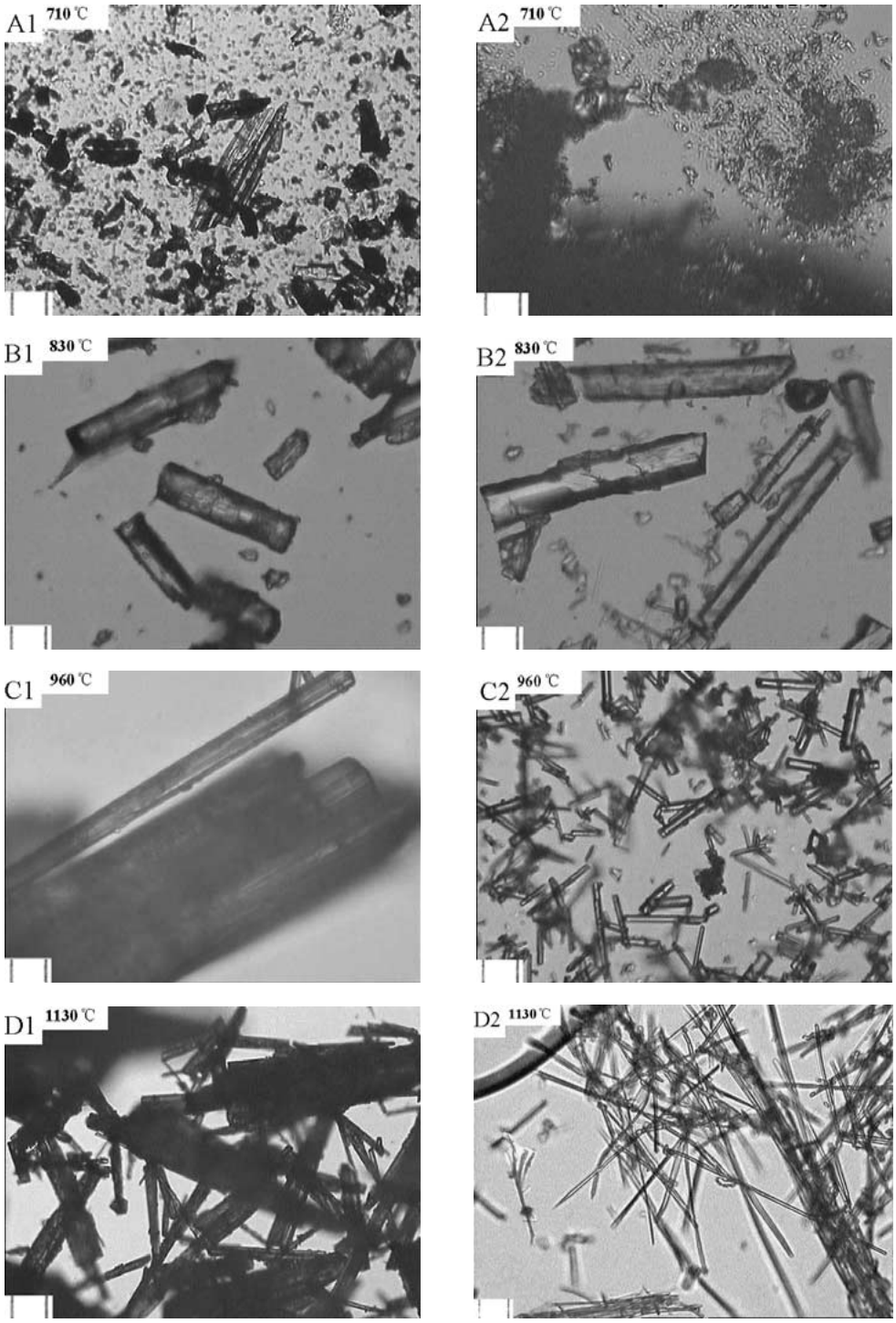

Figure 1 Micrographs showing the morphology and the structure of sinters and crystal products generated at different reaction stages. The size unit is 10 μm. A1, B1, C1 and D1are sinters dispersed in ethanol. A2, B2, C2 and D2 are the dispersed sinters leached by boiling water.

and D2 are $K_2Ti_6O_{13}$ whiskers sharing the similar morphologic and structural differences with those between C1 and C2. Furthermore, it can be seen that D2 still keep some undispersed bunch $K_2Ti_6O_{13}$ whiskers representing the whisker structure of $K_2Ti_6O_{13}$ sinters of D1 after dissolving the coated non-crystalline hydrosoluble products in hot water. Also, $K_2Ti_6O_{13}$ whiskers of D2 are much smaller than $K_2Ti_4O_9$ of C2 in diameter. A detailed microstructure study on $K_2Ti_6O_{13}$ sinters of D1 is shown in Fig. 2.

In Fig. 2 a is a bulk sinter leanched in boiling water for two hours. Fig. 2b is the whisker sheaf separated from the unleanched bulk sinter and a single whisker (in the circle of Fig. 2b) has been partly split from the body of the bunch on its right side. The magnified image for the single whisker is shown in Fig. 2c. Fig. 2b and c are both imaged in ethanol and no hydrosoluble product in them is removed.

In Fig. 2c shows that the single whisker is composed of the surface wrappage and the core whisker, indicating that Fig. 2b is composed of the whisker sheaves in which whiskers are isolated to each other by the hydrosoluble surface wrappage. After leaching the bulk sinter in water at 90°C for two hours to tenderly dissolve the hydrosoluble surface wrappage, the whisker structure of sinters is shown as Fig. 2a. It is found that

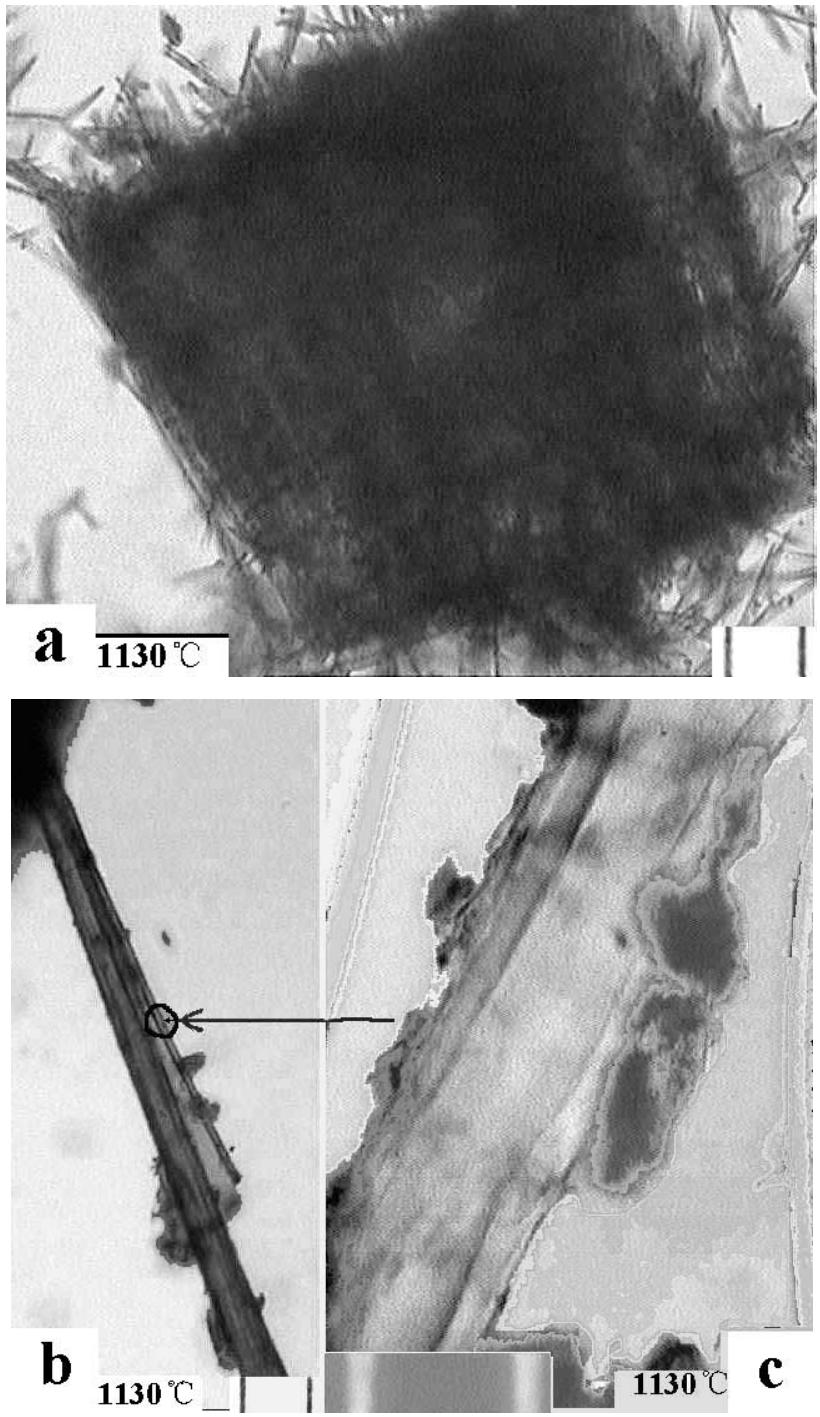

Figure 2 Microstructural study on sinters synthesized at 1130°C. Size unit is 1 μm for (c) and 10 μm for (a) and (b). Sinter in (b) is separated from a bulk sinter which was then leached in boiling water for two hours and shown as (a). A magnified image for a single whisker sinter in the circle of (b) is shown as (c).

the sheaf-like whiskers were neither broken nor dispersed and the places of wrappage in sinters are still left in Fig. 2a.

Fig. 3 shows SEM micrographs of sinters and corresponding whiskers in them. 4PTFa and 6PTFa are SEM images of sinters of C1 and D1, respectively. 4PTFb and 6PTFb are SEM images of whiskers of C2 and D2, respectively.

In Fig. 3 sinters of 4PTFa has the regular concavo-convex surface and are covered by the surface wrappage. The convex places represent the $K_2Ti_4O_9$ whiskers. The concave surface is the solid melt formed from the liquid melt accumulating in the places between two adjacent $K_2Ti_4O_9$ whiskers during the heating calcination, which is caused by the volume shrink as the liquid melt converts into solid melt after the rapid cooling in air. After removing the surface wrappage in 4PTFa in hot water, we obtained the layer-by-layer whiskers as shown in 4PTFb, which also further indicates that the microstructure of sinters of 4PTFa is composed of layered-by-layered whiskers and the hydrosoluble solid melt. 6PTFa is sinters with structure similar to that of 4PTFa. The edge of 4PTFb whiskers is rectangular with a large ratio of the length to the width and the edge of 6PTFb whiskers is close to square. Also, the diameter of 6PTFb is larger than that of 4PTFb, indicating that there is more liquid melts covering on the surface of 6PTFb.

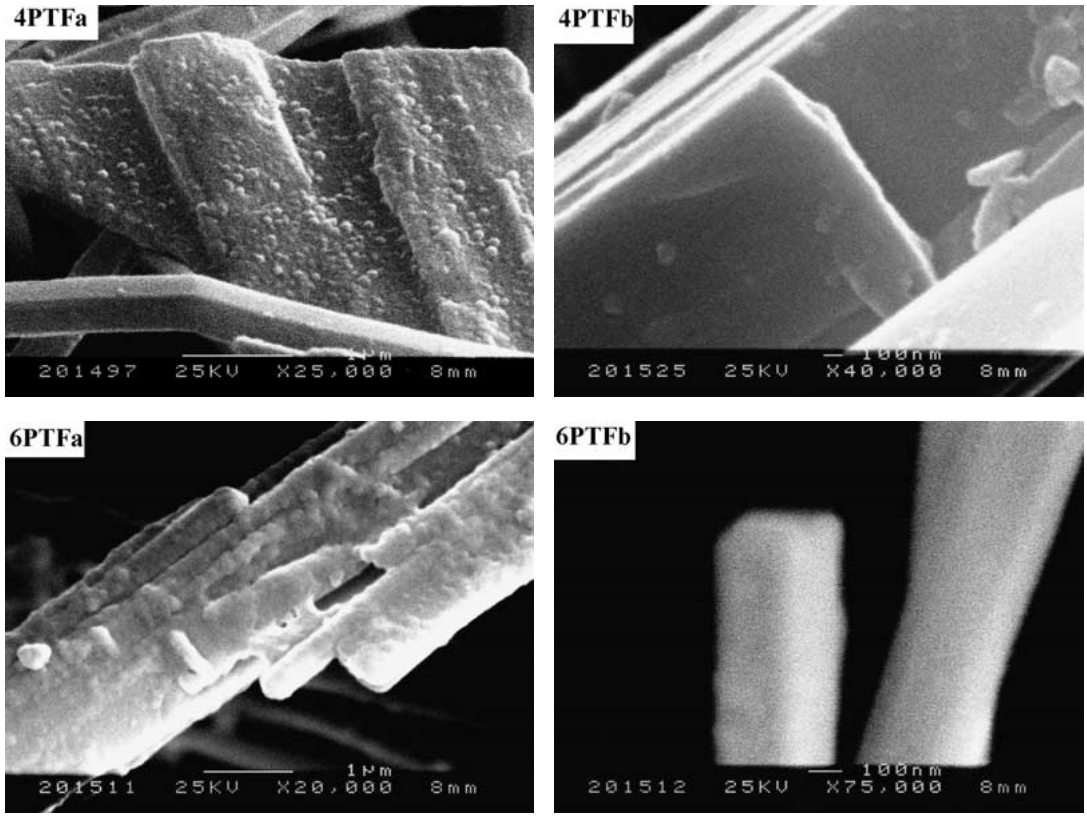

Figure 3 SEM micrographs of sinters and whiskers of $K_2Ti_4O_9$ and $K_2Ti_6O_{13}$. 4PTFa and 4PTFb are $K_2Ti_4O_9$ sinter and $K_2Ti_4O_9$ whisker, respectively; 6PTFa and 6PTFb are $K_2Ti_6O_{13}$ sinter and $K_2Ti_6O_{13}$ whisker, respectively.

Fig. 4 shows both E1 and F1 are bulk sinters and both E2 and F2 are the crystal products dispersed in boiling water. No whiskers are seen in them.

4. Discussion

4.1. Morphodifferentitation and growth of potassium titanates

Table I shows that crystal products in sinters generated at different reaction stages in heating process have different chemical components. However, phase transformations and non-crystal products appearing in the heating calcination can be illustrated in the phase diagram [28] as shown in Fig. 5.

In the phase diagram, for staring materials with the TiO_2/K_2O molar ratio of 3.0 phase transformations and reactions in area A, B, and C in the heating process at $T > 800°C$ are processed along the broken line as shown in Fig. 5, and the step-by-step reactions are listed as follows.

$$K_2CO_{3(solid)} \xrightarrow{T < 828°C} K_2O_{(solid)} + CO_{2(gas)} \quad (1)$$

$$TiO_{2(solid)} + K_2O_{(solid)} \xrightarrow{828°C} K_2Ti_2O_{5(solid)} \quad \text{(area A)} \quad (2)$$

$$K_2Ti_2O_{5(solid)} \xrightarrow{952°C} K_2Ti_4O_{9(solid)} + K_2O - \text{rich phase}_{(liquid)} \quad \text{(area B)} \quad (3)$$

$$K_2Ti_4O_{9(solid)} \xrightarrow{1122°C} K_2Ti_6O_{13(solid)} + K_2O - \text{rich phase}_{(liquid)} \quad \text{(area C)} \quad (4)$$

In Fig. 5 K_2O-rich liquid phase appears at $T > 926°C$ in area D. According to the lever rule of the phase diagram with the increase of the reaction temperature more K_2O-rich liquid phase generates in the succedent reaction, meanwhile the quantity of $K_2Ti_4O_9$ generated decreases. The $K_2Ti_4O_9$ is converted to $K_2Ti_6O_{13}$ at $T > 1114 \pm 15°C$, associating with the emergence of much more K_2O-rich liquid phase when comparing with the former conversion process from $K_2Ti_2O_5$ to $K_2Ti_4O_9$.

Table II lists sinter components, phase diagram analysis results and the morphologies of the samples of A–F.

From Table II, it can be found that the wrappage on the whisker surface are all K_2O-rich liquid phase melt. The morphodifferentitation and growth of potassium titanates in heating calcination thus is illustrated as shown in Fig. 6.

For the slow-cooling calcination starting from $K_2Ti_6O_{13}$ generated at 1130°C phase diagram shows the corresponding reactions and phase transformations. The chemical components and the microstructural evolutions appearing in this process have been reported experimentally by Lee [23] and Fujiki [24]. Actually, the rod-like $K_2Ti_6O_{13}$ particles in their papers are $K_2Ti_6O_{13}$ whiskers as shown in Fig. 1. D1 and Fig. 1. D2. Shimizu [25] reported the synthesis conditions of the potassium titanates by experiments, which can be predicted by the phase diagram.

4.2. Role of K_2O-rich liquid phase for the formation and growth of whiskers

4.2.1. On $K_2Ti_4O_9$ whiskers

Knowing from the phase diagram, the $K_2Ti_4O_9$ whiskers and the K_2O-rich liquid phase appear at

TABLE II Morphology and chemical components of A–F

Sample[a]		TiO_2/K_2O molar ratio	React. temp. (°C)	Symbol	Chem. comp.	Morphology (Exp.)
A	A1	3.0	710	Fig. 1.A1	$TiO_2 + K_2CO_3$	Gain aggregation
	A2			Fig. 1.A2	TiO_2	Gains
B	B1	3.0	830	Fig. 1.B1	$K_2Ti_2O_5$	Single crystal
	B2			Fig. 1.B2	$K_2Ti_2O_5$	Single crystal
C	C1	3.0	960	Fig. 1.C1 and Fig. 3. 4PTFa	$K_2Ti_4O_9$ + Liquid[a]	Surface-wrapped whisker sheaves
	C2			Fig. 1.C2 and Fig. 3. 4PTFb	$K_2Ti_4O_9$	Clean whisker
D	D1	3.0	1130	Fig. 1.D1, Fig. 2b, Fig. 2c and Fig. 3. 6PTFa	$K_2Ti_6O_{13}$ + Liquid[a]	Surface-wrapped whisker sheaves
	D2			Fig. 1.D2, Fig. 2a and Fig. 3. 6PTFb	$K_2Ti_6O_{13}$	Clean whisker
E	E1	3.9	960	Fig. 4.E1	$K_2Ti_4O_9$	Bulk sinter
	E2			Fig. 4.E2	$K_2Ti_4O_9$	Particle
F	F1	5.9	1130	Fig. 4.F1	$K_2Ti_6O_{13}$	Bulk sinter
	F2			Fig. 4.F2	$K_2Ti_6O_{13}$	Particle

[a]Hydrosoluble K_2O-rich phase.

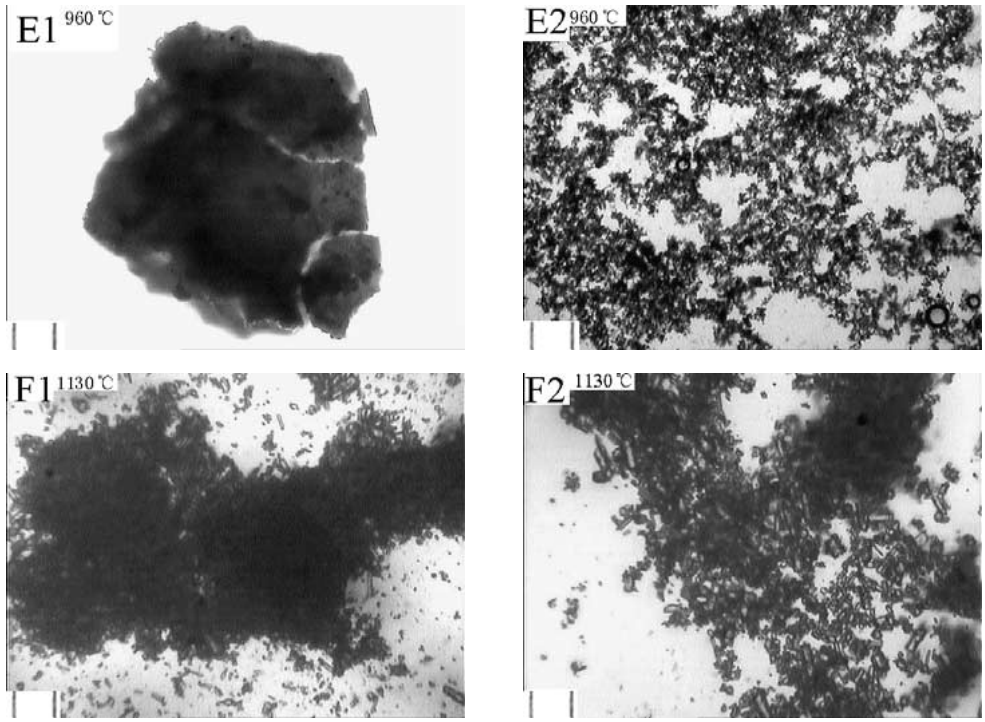

Figure 4 Micrographs of E1, E2, F1 and F2 showing the sinter structure and the morphology of crystal products synthesized from the starting materials with different TiO_2/K_2O molar ratio. The size unit is 10 μm. E1 ($K_2Ti_4O_9$ sinter) and F1 ($K_2Ti_6O_{13}$ sinter) were dispersed in ethanol. E2 ($K_2Ti_4O_9$ grains) and F2 ($K_2Ti_6O_{13}$ grains) were leached by boiling water.

the same time at 926°C in heating calcinations and the phase transformation between the K_2O-rich liquid phase and the solid $K_2Ti_4O_9$whiskers will taken place at $T > 926$°C.

$K_2Ti_2O_5$ single crystals of B2 without liquid phase are generated at 830°C by the reaction expressed by Equation 2. However, hydrosoluble solid melt converted from K_2O-rich liquid phase coats on the $K_2Ti_4O_9$ whisker surface, which makes the sinters taking on whisker sheaves as shown in Fig. 1. C1. The whisker sheaves can be broken into $K_2Ti_4O_9$ whiskers as shown in Fig. 1. C2 in hot water. On the other hand, $K_2Ti_4O_9$ whisker sheaves share the close size with those of $K_2Ti_2O_5$ single crystals. These indicate that $K_2Ti_4O_9$ whiskers are evolved or formed in $K_2Ti_2O_5$ single crystals. The $K_2Ti_4O_9$ sinter has the regular concavo-convex surface and whiskers in it are wrapped by the K_2O-rich liquid phase generated in the $K_2Ti_2O_5$. These also indicate that the K_2O-rich liquid phase splits the $K_2Ti_2O_5$ single crystals into $K_2Ti_4O_9$ whiskers and then accumulates in the places between two adjacent $K_2Ti_4O_9$ whiskers. After dissolving the solid melt in hot water, we easily obtained dispersed layer-by-layer $K_2Ti_4O_9$ whiskers of 4PTFb as shown in Fig. 3 and of C2 as shown in Fig. 1 from the $K_2Ti_4O_9$ sinters of 4PTFa as shown in Fig. 3 and of C1 as shown in Fig. 1. This process is expressed by Equation 3.

$K_2Ti_4O_9$ whiskers are firstly formed in $K_2Ti_2O_5$ single crystals by the split effect of K_2O-rich liquid melt generated in the $K_2Ti_2O_5$ single crystal. The K_2O-rich liquid melt wraps on the $K_2Ti_4O_9$whisker surface and isolates the whiskers.

4.2.2. On $K_2Ti_6O_{13}$ whiskers

With the increase of the calcination temperature over 1114 ± 15°C $K_2Ti_6O_{13}$ whiskers are generated from

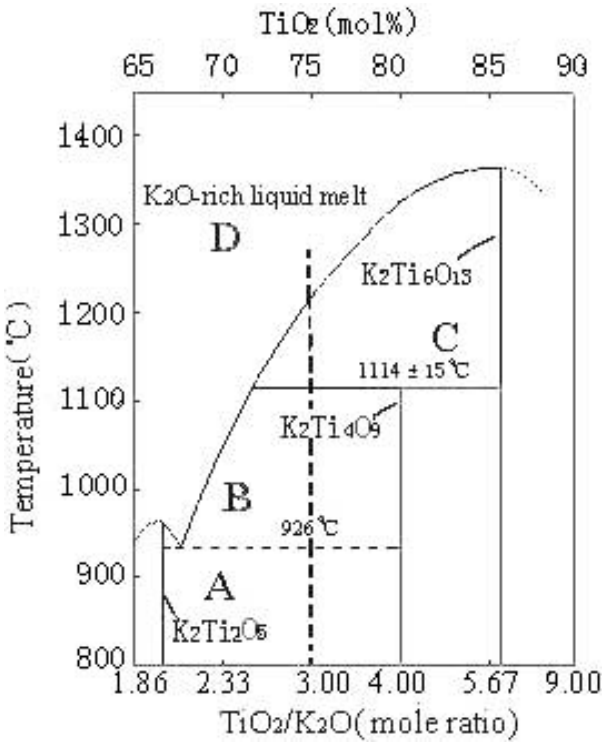

Figure 5 Phase diagram of the K_2O–TiO_2–$K_2O \cdot nTiO_2$ ($n = 2$, 4 and 6) system [28].

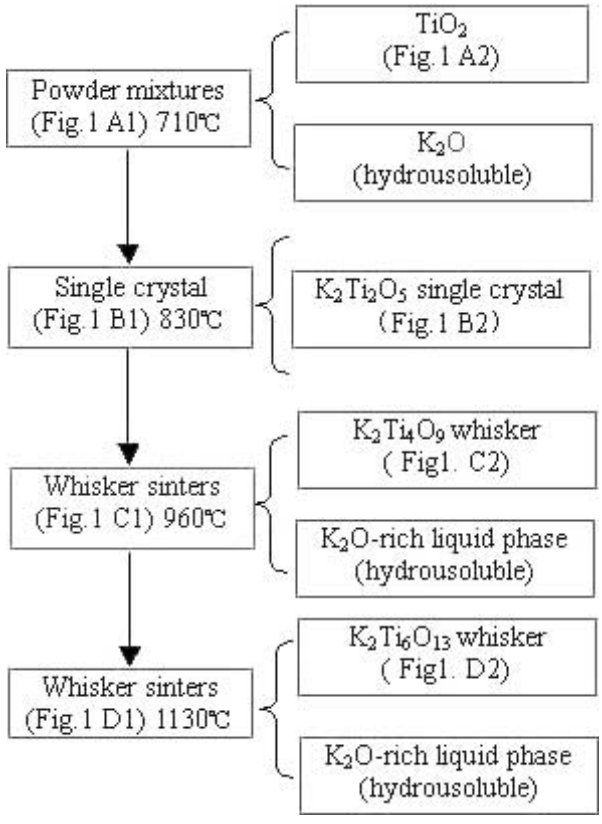

Figure 6 Shematic diagram of the morphodifferentitation and growth of potassium titanate whiskers.

$K_2Ti_4O_9$ whiskers accompanying by the continuous melt of K_2O-rich liquid phase.

The structure and the morphology of $K_2Ti_6O_{13}$ sinters are similar to those of $K_2Ti_4O_9$ sinters. The diameter of $K_2Ti_6O_{13}$ is smaller than that of $K_2Ti_4O_9$ whisker. With the increase of the reaction temperature the size decrease in diameter of whiskers is processed, which are dictated by this fact that is during the heating calcination the quantity of the K_2O-rich liquid phase generated increases and the amount of the solid phase (whiskers) decreases simultaneously knowing from the phase diagram. Morphologic and structural analysis to Fig. 2 also presents the experimental evidence showing the orientation melt of rich-K_2O liquid phase from whisker in diameter. Here, corresponding crystal structures of whiskers change from the layered crystal structure of $K_2Ti_4O_9$ to the tunnel crystal structure of $K_2Ti_6O_{13}$ [32–35], which might be the main fundamental reason causing the formation and growth of different types of potassium titania whiskers and further contributing to the morphologic change such as the different cross-section morphologies of $K_2Ti_4O_9$ whiskers and $K_2Ti_6O_{13}$ whiskers.

4.2.3. On sinter structure

The quantity of K_2O-rich liquid phase and its orientation melt in diameter play key roles in determining the formation and growth of potassium titanate whiskers, which results in the generation of sinters and corresponding crystal products with different structure, morphology and size.

K_2O-rich liquid melt plays key role for the formation and growth of the $K_2Ti_4O_9$ whiskers and the $K_2Ti_6O_{13}$ whiskers. The sinters of $K_2Ti_4O_9$ and $K_2Ti_6O_{13}$ are all composed of the whisker sheaves glued by the liquid melt. $K_2Ti_4O_9$ whiskers of C2 in their sinters of C1 are firstly formed in $K_2Ti_2O_5$ single crystals of B2, and then $K_2Ti_4O_9$ whiskers are converted into $K_2Ti_6O_{13}$ whiskers of D2 with smaller diameter at a higher reaction temperature. If little liquid melt is generated to split the bulk sinter and to isolate the whiskers, the whisker cannot form and grow. Starting materials using to prepare E and F have the TiO_2/K_2O molar ratios of 3.9 and 5.9, respectively. When the reaction temperatures are 960°C and 1130°C, respectively, there is little liquid melt generated knowing form the phase diagram. Experimental results in Fig. 4 also confirm that no whiskers generate for E and F. As a result, suitable amount of the liquid melt are needed for the formation and growth of whiskers.

Knowing from phase diagram the K_2O-rich liquid also participates in the reaction and growth of potassium titanates in the cooling process starting at higher reaction temperatures (>1130°C), which has been observed well by Lee [23] experimentally.

4.3. "Liquid melt inducing" model

"Liquid melt inducing" model for the formation and growth of different types of potassium titanate whiskers is illustrated schematically in Fig. 7. In Process 1, the surfactant is used to assembly the well-mixed precursor, the anatase-K_2CO_3 inclusion containing the nano TiO_2 powders coated by K_2CO_3 crystallized from the solution. In Process 2, the decomposable $K_2Ti_2O_5$ single crystals providing the matrix materials for the formation of $K_2Ti_4O_9$ whiskers are generated by the solid-solid sinter calcination. In Process 3, the orientation

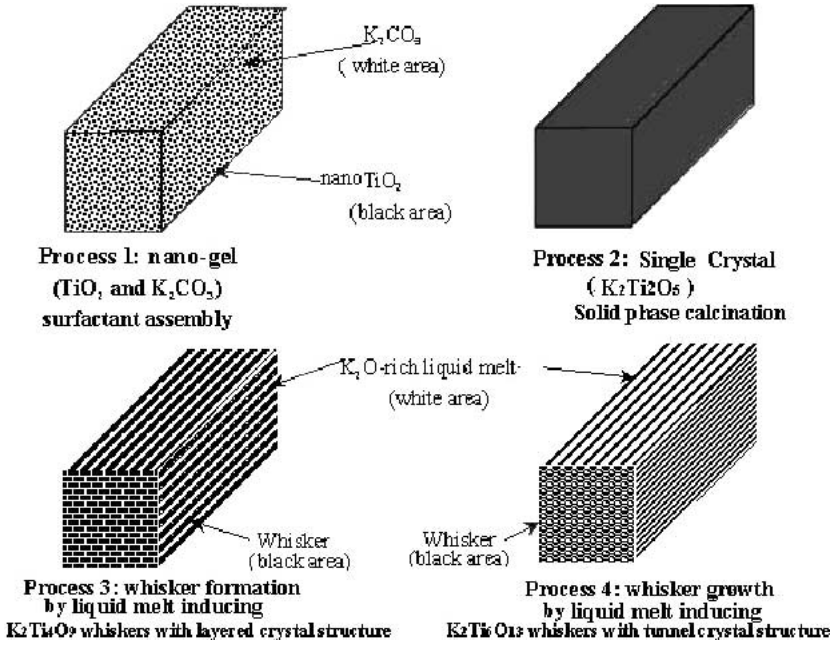

Figure 7 Schematic representation of a generalized "liquid melt inducing" model.

melt of the K_2O-rich liquid melt splits the decomposable $K_2Ti_2O_5$ single crystals into layer-by-layer $K_2Ti_4O_9$ whiskers with layered crystal structure. Liquid melt covers on the whisker surface to form the sinters with sheaf whisker structure. Process 4 is processed at a higher reaction temperature. The K_2O-rich liquid melt melts and aggregates in the splits and the spaces among solid $K_2Ti_6O_{13}$ whiskers. When comparing with Process 3 the whiskers with tunnel crystal structure evolves from the former $K_2Ti_4O_9$ whiskers with layered crystal structure and much more liquid melt generated induces the size decrease of the $K_2Ti_6O_{13}$ whiskers in diameter.

In fact, the other alkali titanium-matrix synthetic whiskers or the mixed metal titanates [2] with the similar layered and tunnel crystal structure share the same formation and growth mechanism as that of potassium titanate whiskers.

5. Conclusion

The formation and growth of different types of potassium titanium whiskers were observed and studied, which provided the control method for the morphologic and size of products. K_2O-rich liquid phase plays a key role for the formation and growth of potassium titanium whiskers in the heating calcination. $K_2Ti_4O_9$ whiskers in sinters firstly evolve in large $K_2Ti_2O_5$ single crystals at 960°C, and $K_2Ti_4O_9$ whiskers are converted into $K_2Ti_6O_{13}$ whiskers with smaller diameter at higher calcination temperature over 1130°C. A suitable quantity of K_2O-rich liquid melt results in the synthesis of high quality potassium titanate whiskers with good whisker morphology and size at the TiO_2/K_2O molar ratio of 3.0.

Acknowledgments

Authors thank the National Natural Science Foundation of P. R. China (No. 29376244), Natural Science Foundation of Jiangsu Province of P. R. China (BJ98060) and the Outstanding Youth Fund of National Natural Science Foundation of P. R. China (29925616).

References

1. H. KONUCHI and Y. NARITA, *Zeolite (Japan)* **19**(3) (1992) 103.
2. A. CLEARFIELD, *Chem. Rev.* **88** (1988) 125.
3. J. LU and X. LU, *J. Appl. Polym. Sci.* **82**(2) (2001) 368.
4. S. C. TJONG and Y. Z. MENG, *Polymer* **40** (1999) 7275.
5. J. HOMENY, in "Ceramic Matrix Composites," edited by W. Reachard (Blackie, Glasgow, UK, 1993) p. 240.
6. S. TARUTA, S. HIROKAWA, H. KAWAMURA and N. TAKUSAGAWA, *J. Ceramic Soc. of Japan* **105**(12) (1997) 1158.
7. P. BALDUS, M. JANSEN and D. SPORN, *Science* **285** (1999) 699.
8. H. IZAWA, S. KIKKAWA and M. KOIZUMI, *J. Phys. Chem.* **86** (1982) 5023.
9. T. SASAKI, M. WATANABE, Y. KOMATSU and Y. FUJIKI, *Inorg. Chem.* **24** (1985) 2265.
10. C. LEE, M. UM and H. KUMAZAWA, *J. Amer. Ceramic Soc.* **85**(5) (2000) 1098.
11. N. OHTA and Y. FUJUIKI, *Yogyo-Kyokai-Shi* **88**(1) (1980) 9.
12. N. BAO, X. LU, X. JI, X. FENG and J. XIE, *Fluid Phase Equilibria* **193**(1–2) (2002) 229.
13. M. SANDO, A. TOWATA and A. TSUGE, in "Ceramic Transactions," Vol. 22, edited by S. Hirano, G. L. Messing and H. Hausner (American Ceramic Society, Westerville, OH, 1991) p. 101.
14. H. M. LIN, C. H. KENG and C. Y. TUNG, *Nanostructured Materials* **9** (1997) 747.
15. A. M. KATAYAMA, H. HASEGAWA, T. NODA, T. AKIBA and H. YANAGIDA, *Sensors and Actuators B* **2** (1992) 143.
16. S. KIKKAWA, F. YASUDA and M. KOIZUMI, *Mat. Res. Bull.* **20** (1985) 1221.
17. K. WANG, Y. HSIEH, R. KO and C. CHANG, *Environment International* **25**(5) (1999) 671.
18. C. LIU, N. BAO, Z. YANG and X. LU, *Chin. J. of Catalysis* **22** (2001) 215.
19. S. YIN and T. SATO, *Ind. Eng. Chem. Res.* **39** (2000) 4526.
20. T. SASAKI, S. NAKANO, S. YAMAUCHI and M. WATANABE, *Chem. Mater.* **9** (1997) 602.
21. C. A. MARKIN, *Inorg. Chem.* **39** (2000) 2258.
22. J. YANG, G. H. CHENG, J. H. ZENG, S. H. YU, X. M. LIU and Y. T. QIAN, *Chem. Mater.* **13** (2001) 848.

23. J. LEE, K. LEE and H. KIM, *J. Mater. Sci.* **31** (1996) 5493.
24. Y. FUJIKI, *Yogyo-Kyokai-Shi* **90**(10) (1982) 76.
25. T. SHIMIZU, H. YANAGIDA and K. HASHIMOTO, *ibid.* **86**(8) (1978) 339.
26. F. C. FRANK, *Phil. Mag.* **44** (1953) 854.
27. R. S. WAGNER and W. C. ELLIS, *J Appli. Phys.* **100** (1964) 271.
28. O. SCHMITZ-DUMONT and H. RECKHARD, in "Phase Diagrams for Ceramists," edited by E. M. Levin, C. R. Robbins and H. F. McMurdie (American Ceramic Society, Columbus, OH, 1964) p. 87.
29. C. BAMBERGER, G. BEGUN and S. MACDOUGALL, *App. Spectrosc.* **44** (1990) 30.
30. U. EASTEAL, *J. Inorg. Nucl. Chem.* **35** (1973) 3956.
31. E. ANDERSON, I. ANDERSON and E. SKOU, *Solid State Ionics* **27** (1988) 181.
32. M. DION, Y. PIFFARD and M. TOURNOUX, *J. Inorg. Nucl. Chem.* **40**(5) (1978) 917.
33. S. ANDERSSON and A. D. WADSLEY, *Acta. Crystallogr.* **15** (1962) 194.
34. H. CID-DRESDNER and M. J. BUERGER, *Z. Krist.* **117** (1962) 411.
35. H. IZAWA, S. KIKKAWA and M. KOIZUMI, *J. Solid State Chem.* **69** (1987) 336.

Received 2 February 2001
and accepted 28 February 2002